Interactions of Cyclins with Cyclin-Dependent Kinases: A Common Interactive Mechanism†

Frederic Heitz,‡ May C. Morris,‡ Didier Fesquet, Jean-Claude Cavadore, Marcel Dorée, and Gilles Divita*

Centre de Recherches de Biochimie Macromoleculaire, CNRS, BP 5051, 1919 Route de Mende, 34033 Montpellier, Cedex 1, France

Received September 17, 1996; Revised Manuscript Received January 27, 1997⊗

ABSTRACT: The formation of cdk−cyclin complexes has been investigated at the molecular level and quantified using spectroscopic approaches. In the absence of phosphorylation, cdk2, cdc2, and cdk7 form highly stable complexes with their "natural" cyclin partners with dissociation constants in the nanomolar range. In contrast, nonphosphorylated cdc2−cyclin H, cdk2−cyclin H, and cdk7−cyclin A complexes present a 25-fold lower stability. On the basis of both the structure of the cdk2−cyclin A complex and on our kinetic results, we suggest that interaction of any cyclin with any cdk involves the same hydrophobic contacts and induces a marked conformational change in the catalytic cleft of the cdks. Although cdks bind ATP strongly, they remain in a catalytically inactive conformation. In contrast, binding of the cyclin induces structural rearrangements which result in the selective reorientation of ATP, a concomitant 3-fold increase in its affinity, and a 5-fold decrease of its release from the active site of cdks.

Progression of the cell cycle in higher eukaryotes is governed by members of the cyclin-dependent kinase family (cdks).[1] These heterodimeric complexes are composed of a catalytic protein kinase subunit (cdk) and of a regulatory cyclin partner. Eight members of the cdk family (cdk1−cdk8) and nine cyclins (A−I) have been identified so far [reviews: Pines (1993), Dunphy (1994), Sherr (1994), and Morgan (1995) and references therein]. Cdk protein kinases are closely related in size, ranging from 30 to 40 kDa, and share at least 40% sequence homology. They contain a highly conserved catalytic core of 300 residues which is also present in all other eukaryotic protein kinases (Hanks et al., 1988). Cyclin subunits named after their cyclical pattern of accumulation and destruction throughout the cell cycle vary importantly in size (30−80 kDa) but are nevertheless fairly homologous within particular domains, in particular, a 100 amino acid stretch: the cyclin box (Pines, 1993; Hunter & Pines, 1994). Formation of cdk−cyclin complexes is regulated both by protein/protein interactions and by reversible phosphorylation. Monomeric cdk subunits do not exhibit protein kinase activity whereas association with a cyclin partner confers basal kinase activity to the cdk−cyclin complex and further promotes phosphorylation of the cdk on the conserved threonine 160 (amino acid position in cdk2) by the cdk activating kinase complex (CAK) (Fesquet et al., 1993; Poon et al., 1993; Solomon et al., 1993; Fisher & Morgan 1994; Solomon 1994), which finally renders the complex fully active (Morgan, 1995; Russo et al., 1996). Moreover, the cyclin subunit modulates substrate specificity and cellular localization of the kinase complex (Pines & Hunter, 1991; Kobayashi et al., 1992; Maridor et al., 1993).

Determination of the X-ray cristallographic structures of cdk2 (Debondt et al., 1993), mitogen-activated protein kinase (MAPK) (Zhang et al., 1994), cyclic-AMP-dependent protein kinase (cPKA) (Knighton et al., 1991), the tyrosine kinase domain of the human insulin receptor (Hubbard et al., 1994), and casein kinase 1 (Longenecker et al., 1996; Xu et al., 1995) has revealed a common structural organization of protein kinases in two domains: a small lobe containing the nucleotide binding site and a large lobe corresponding in part to the protein substrate binding site. ATP binds in a deep cleft located between the two lobes which contains well-conserved catalytic residues.

Despite these common structural features, cdks present differences with other protein kinases in their mechanism of regulation. The structure of cyclin A has revealed a two-helical-domain organization, each domain containing five α-helices which is characteristic of cyclins (Brown et al., 1995; Jeffrey et al., 1995). This characteristic cyclin helix fold has indeed been predicted in all cyclins, but also in other cyclin-like proteins, although they only share little sequence similarity (Bazan, 1996), and surprisingly, in transcription factor TFIIB (Bagby et al., 1995; Nikolov et al., 1995).

The recent determination of the structure of unphosphorylated and phosphorylated cdk2−cyclin A complexes has been an important step in the understanding of the mechanism of cdk2 activation, which takes place upon binding to its cyclin subunit (Jeffrey et al., 1995; Russo et al., 1996). The cyclin subunit binds to one side of the catalytic cleft of cdk2 and interacts with the two lobes of cdk2, thus forming a large continuous hydrophobic protein/protein interface. The main structural motifs involved in this interface are the α1-helix, which contains the characteristic PSTAIRE sequence and the T-loop of cdk2, and the α3, α4, and α5-helices of the first helix fold of cyclin A. Weaker interactions with cyclin A take place in the N-terminal β-sheet and the

† This work was supported by the CNRS and by a grant from the Association pour la Recherche contre le Cancer (ARC, Contract 1244).

* To whom correspondence should be addressed. Tel.: (33) 67 61 33 92. Fax: (33) 67 52 15 59. E-mail: gilles@merlin.crbm.cnrs-mop.fr.

‡ These authors contributed equally to this work.

⊗ Abstract published in *Advance ACS Abstracts,* April 1, 1997.

[1] Abbreviations: cdk, cyclin-dependent kinase; CAK, cdks activating kinase; MAPK, mitogen-activated protein kinase; cPKA, cyclic-AMP-dependent protein kinase; CK1, casein kinase 1; mant-ATP and mant-ADP, *N*-methylanthraniloyl-adenosine di and triphosphate; GST, glutathione *S*-transferase.

S0006-2960(96)02349-5 CCC: $14.00

C-terminal lobe of the cdk2 which are stabilized by a network of hydrogen bonds. Comparison of the structure of unbound cyclin A with that of cyclin A complexed to cdk2 reveals that no significant conformational changes occur within cyclin A upon formation of the cdk−cyclin complex. In contrast, cyclin binding to cdk2 induces a conformational change of cdk2 which is essential for its activation. It involves a rotation of the PSTAIRE helix about its axis thus moving it into the catalytic site and a positional switch of the T-loop, which promotes phosphorylation of Thr160 by CAK. The most important feature of this conformational change is the reconfiguration of the ATP binding site which moves the $\beta-\gamma$ phosphate bond of ATP into a position which favors nucleophilic attack by the substrate (Jeffrey et al., 1995). Finally, phosphorylation of Thr160 induces additional conformational changes in the T-loop and in the C-terminal lobe of cdk2 which strengthen the contact between cdk2 and cyclin A and affect the orientation of the putative substrate binding site of cdk2 (Russo et al., 1996).

Further understanding of the molecular basis of cell division requires appropriate investigations of the molecular features and structural interactions between cyclins and cdks. In this study, we have developed powerful tools for the direct investigation of the mechanism of formation of cdk−cyclin complexes. Our results show that highly stable cdk−cyclin complexes can form *in vitro* without requiring prior phosphorylation. On the basis of the comparative characterization of three cdks, cdk2, cdc2, and cdk7, with respect to their association with cyclin partners, we propose a common mechanism of interaction of cyclin subunits close to the ATP binding pocket of cdks. The cyclin strongly modifies the catalytic cleft of the cdk into a conformation which places the ATP appropriately for the catalysis.

EXPERIMENTAL PROCEDURES

Materials. Restriction enzymes, Klenow, and T4 DNA ligase were obtained from Promega Corp. Ni^{2+}−nitrilotriacetic acid−agarose was from Quiagen Inc. The TSK-250 and TSK-125 columns were from Bio-Rad. ADP and ATP were purchased from Boehringer. The purity and stability of the nucleoside and nucleotide analogues were checked by reverse phase HPLC. Mant-derivative nucleotides were synthetized as described by Hiratsuka (1983) and purified according to John et al. (1990). Endogenous nucleotides were titrated, after thermal denaturation, by HPLC on a C18 reverse phase column (Divita et al., 1993a).

Cloning and Protein Expression and Preparation. The human-cdc2 ORF was excised from the pTZ19B-cdc2 construct by *Nde*I digestion, made blunt with Klenow, and subcloned into the *Sma*I site of the pQE30 vector (Quiagen). The *Xenopus* cyclin H cDNA was subcloned from pcDNA3 cycH into the pQE31 vector to produce a N-terminally tagged cyclin H (Quiagen).

GST−cdk2 and GST−cdk7 as well as cyclin A were overexpressed in *Escherichia coli* and purified to homogeneity as previously described (Lorca et al., 1992; Labbé et al., 1994; Devault et al., 1995). The GST tag moiety was removed with factor Xa or thrombin and the proteins were purified further by size exclusion chromatography. N-terminal polyHis-tagged cyclin H and cdc2 were obtained by overexpression in *E. coli* as soluble proteins. Cultures were grown at 37 °C in LB medium (10 g/L bacto-tryptone, 5 g/L bacto-yeast extract, 10 g/L NaCl) containing 50 μg of ampicillin/mL to A_{600} of 0.7−0.8 followed by induction with IPTG to a final concentration of 2 mM for 3 h. Cells were harvested by centrifugation and disrupted by sonication in buffer A [50 mM K_2HPO_4, 12 mM KH_2PO_4 (pH 7.2), 200 mM NaCl, 1 mM EDTA] containing 20 mM imidazole at 4 °C. After high-speed centrifugation, the supernatant was applied onto a Ni^{2+}−nitrolotriacetic acid−agarose column (Pharmacia) equilibrated with the buffer A . The His_6-tagged cyclin H and cdc2 was eluted with buffer A containing 300 mM imidazole and analyzed by SDS−PAGE (10%) (Laemmli, 1970). Fractions containing at least 95% of purified cyclin H or cdc2 were concentrated and dialyzed against buffer A containing 50% glycerol and stored at −80 °C.

Fluorescence Experiments. Fluorescence measurements were performed at 25 °C using a Spex II fluorolog spectrofluorometer, with spectral band-passes of 2 and 8 nm for excitation and emission, respectively. The intrinsic tryptophan fluorescence of the different cdks (0.1−1.0 μM protein) was measured in a fluorescence buffer containing 50 mM Tris-HCl (pH 7.5), 50 mM KCl, 5% glycerol, and 2 mM EDTA (or 5 mM excess of $MgCl_2$). Proteins were incubated 30 min in fluorescence buffer before starting the experiments and all measurements were corrected as already described (Divita et al., 1993b). Excitation was performed at 290 nm, and the emission spectrum was scanned from 310 to 450 nm. The binding of nucleotides was monitored by the quenching of the intrinsic tryptophan fluorescence of cdks at 340 nm upon excitation at 295 nm. A fixed concentration of cdks was titrated by increasing the concentration of ATP, ADP, or labeled nucleotide. The binding of mant-nucleotides to cdks or cdk−cyclin complexes was monitored by the enhancement of the mant-group fluorescence at 450 nm upon excitation at 340 nm (John et al., 1990). Fitting of titration curves was accomplished using the Grafit software (Erithacus software Ltd) with the following equation:

$$F = F_{ini} - \{(\Delta F)[(E_t + L + K_d) - [(E_t + L + K_d)^2 - 4E_tL]]^{1/2}\}/2E_t \quad (1)$$

where F is the relative fluorescence intensity, F_{ini} is the relative fluorescence intensity at the beginning of the titration, ΔF is the variation of the fluorescence intensity between the initial value and at saturating concentrations of substrate (L), E_t is the total concentration of cdks or mant-nucleotide depending on the titration and K_d is the dissociation constant of the enzyme−substrate complex. All the results correspond to the average of four separate experiments with a standard deviation lower than 10% for intrinsic and extrinsic fluorescence titrations.

Size-Exclusion HPLC. Size-exclusion chromatography was performed using two HPLC columns (Bio-Rad) in series TSK-250 followed by TSK-125 (7.5 × 200 mm). The proteins (cyclins and cdks) and cdk−cyclin complexes (0.2−2 μM) were incubated 15 min at 25 °C, then applied and eluted with 150 mM potassium phosphate (pH 6.8 or 7.2) at a flow rate of 0.8 mL/min. This method was used for analytical as well as for preparative experiments. The separated cdk−cyclin complexes were analyzed by SDS−PAGE (Laemmli, 1970).

Measurement of the Interaction between Cdks and Cyclins. The affinities between cdks and cyclins were measured by

two approaches: the direct fluorescence titration of the cdk−mant-ATP complex with different cyclin concentrations and the displacement experiments of mant-ATP using an excess of ATP or ADP. In both cases, mant-ATP−cdk complexes were incubated 15 min in the presence of different cyclin concentrations before starting the experiment.

Interactions between cdks and cyclins were monitored using the enhancement of mant-ATP fluorescence at 430 nm. The mant-ATP−cdk complexes were kept at a constant concentration of 0.2 μM and fluorescence emission was monitored at 430 nm (excitation at 350 nm) as a function of the concentrations of cyclins. The K_d was calculated by fitting the data to a standard quadratic equation.

In the displacement experiments, a cdk−mant-ATP complex concentration of 0.2 μM in fluorescence buffer was incubated in the presence of a 200-fold excess of unlabeled nucleotide and increasing concentrations of cyclins were added. The kinetics of dissociation of the fluorescently labeled nucleotide were monitored by the quenching of mant-fluorescence at 430 nm upon excitation at 350 nm. The dissociation rate constants (k_{obs}) were determined by fitting the data to single exponentials. The k_{obs} values were fitted according to the model described in the Results using the following eq 2 to yield dissociation constants (K_{ds}) of cdks for the corresponding cyclins.

$$k_{obs} = k_{-1} - (k_{-1} - k_{-2}) \frac{([C_0] + [K_0] + K_d) - \sqrt{([C_0] + [K_0] + K_d)^2 - 4[C_0][K_0]}}{2[C_0]} \quad (2)$$

RESULTS

Binding of Nucleotides to Cdks Monitored by Quenching of Intrinsic Fluorescence. All cdks contain three conserved Trp-residues, corresponding to positions 167, 187, and 229 of cdk2 (Figure 1), located in key domains of the kinases (Taylor & Radzio-Andzelm, 1994). The structures of cdk2 (Debondt et al., 1993) and of cdk2 complexed to cyclin A (Jeffrey et al., 1995; Russo et al., 1996) have shown that Trp167 is located in the T-loop close to the essential Thr160 phosphorylation site and to the catalytic site of the kinase. As shown in Figure 2A (curve 1), these Trp-residues confer to cdk2, cdk7, and His_6-cdc2 an important intrinsic fluorescence with emission spectra centered at 334 nm, characteristic of deeply buried Trp-residues. This property offers the potential for investigating the interactions of cdks with their substrates and of other proteins such as cyclins involved in their regulation. In order to exclude an effect of the GST tag on the affinity of cdks for the nucleotide, the same experiments were performed with both tagged and nontagged cdk2 and cdk7, from which the GST tag was cleaved using factor Xa or thrombin and the nontagged kinase was further purified by gel filtration.

The binding of ATP or ADP to cdks produced a marked quenching of intrinsic fluorescence up to 40% for cdk7 and 48% for cdk2 and His_6-cdc2, at saturating concentrations without any shift in the emission spectrum (Figure 2A, curve 2). The titration curves in which a fixed concentration of cdks (0.2 μM) were titrated by increasing the concentration of ATP are monophasic (Figure 2B). The three cdks bound ATP with high affinity and the apparent dissociation

```
        30         40         50         60         70         80
cdc2hu  SEGVPSTAIR EISLLKEVN- --DENNRSNC VRLLDILHA ESKLYLVFEF LDMDLKKYMD
cdk2hu  TEGVPSTAIR EISLLKELN- --HPNIVKLL DV----IHT ENKLYLVFEF LHQDLKKFMD
cdk3hu  MEGVPSTAIR EISLLKELK- --HPNIVRLL DV----VHN ERKLYLVFEF LSQDLKKYMD
cdk4hu  GGGLPISTVR EVALLRRLEA FEHPNVVRLM DVATSRTDR EIKVTLVFEH VDQDLRTYLD
cdk5hu  DEGVPSSALR EICLLKELK- --HKNIVRLH DV----LHS DKKLTLVFEF CDQDLKNF-D
cdk6hu  EEGMPLSTIR EVAVLRHLET FEHPNVVRLF DVTVSRTDR ETKLTLVFEH VDQDLTTYLD
cdk7xe  NDGINRTALR EIKLLQELS- --HPNIIGLL DA----FGH KSNISLVFDF METDLEVIIK

        90         100        110        120        130        140
cdc2hu  RISETGATSL DPRLVQKFTY QLVNGVNFCH SRRIIHRDLK PQNLLIDKEG NLKLADFGLA
cdk2hu  ASALTGIPLP LIKSYL-FQL LQ--GLAFCH SHRVLHRDLK PQNLLINTEG AIKLADFGLA
cdk3hu  STPGSELPLH LIKSYL-FQL LQ--GVSFCH SHRVIHRDLK PQNLLINELG AIKLADFGLA
cdk4hu  KAPPPGLPAE TIKDLMRQFL R---GLDFLH ANCIVHRDLK PENILVTSGG TVKLADFGLA
cdk5hu  SCNG-DLDPE IVKSFL-FQL LK--GLGFCH SRNVLHRDLK PQNLLINRNG ELKLADFGLA
cdk6hu  KVPEPGVPTE TIKDMM-FQL LR--GLDFLH SHRVVHRDLK PQNILVTSSG QIKLADFGLA
cdk7xe  DTSLV-LTPA HIKSYMLMTL Q---GLEYLH HLWILHRDLK PNNLLLDENG VLKLADFGLA

        150        160        170        180        190        200
cdc2hu  RSFGVPLRNY THEIVTLWYR APEVLLGSRH YSTGVDIWSV GCIFAEMIRR -SPLFPGDSE
cdk2hu  RAFGVPVRTY THEVVTLWYR APEILLGCKY YSTAVDIWSL GCIFAEMVTR -RALFPGDSE
cdk3hu  RAFGVPLRTY THEVVTLWYR APEILLGSKF YTTAVDIWSI GCIFAEMVTR -KALFPGDSE
cdk4hu  RIYSYQMAL  TPVVVTLWYR APEVLLQS-T YATPVDMWSV GCIFAEMFRR -KPLFCGNSE
cdk5hu  RAFGIPVRCY SAEVVTLWYR PPDVLFGAKL YSTSIDMWSA GCIFAELANA GRPLFPGNDV
cdk6hu  RIYSFQMALT SV-VVTLWYR APEVLLQSS- YATPVDLWSV GCIFAEMFRR -KPLFRGSSD
cdk7xe  KSFGSPNRIY THQVVTRWYR SPELLFGARM YGVGVDMWAV GCILAELLLR -VPFLPGDSD

        210        220        230        240        250
cdc2hu  IDEIFKIFQ VLGTPNEEVW PGVTLLQDYK STFPRW-KRM DLHKVVPNGEE
cdk2hu  IDQLFRIFR TLGTPDEVVW PGVTSMPDYK PSFPKW-ARQ DFSKVVPPLDE
cdk3hu  IDQLFRIFR MLGTPSEDTW PGVTQLPDYK GSFPKW-TRK GLEEIVPNLEP
cdk4hu  ADQLGKIFD LIGLPPEDDW PRDVSLPR-- GAFPPRGPRP VQ-SVVPEMEE
cdk5hu  DDQLKRIFR LLGTPTEEQW PSMTKLPDYK P-YPMYPATT SLVNVVPKLNA
cdk6hu  VDQLGKILD VIGLPGEEDW PRDVALPRQA --FHSKSAQ- PIEKFVTDIDE
cdk7xe  LDQLTRIFE TLGTPTEEQW PGMSSLPDY- VAFKSFPG-T PLHLIFIAAGD
```

FIGURE 1: Sequence alignment of the human and Xenopus cyclin-dependent kinases. Cdc2hu, human cdc2; cdk2hu, human cdk2; cdk3hu, human cdk3; cdk4hu, human cdk4; cdk5hu, human cdk5; cdk6hu, human cdk6; cdk7xe, xenopus cdk7).

constants (K_d) were calculated to 227 ± 20, 280 ± 20, and 234 ± 30 nM for cdk2, cdk7, and His_6-cdc2, respectively. In contrast, the affinity for ADP was at least 5−10-fold lower than for ATP, with K_d values of 1.4 ± 0.4, 2.7 ± 0.3, and 2.1 ± 0.5 μM for cdk2, cdk7, and His_6-cdc2, respectively (Table 1). The presence of 5 mM excess of Mg^{2+} in the buffer did not modify the affinity of cdks for ATP or ADP. Similar titration patterns were obtained for the GST−cdks with K_d values for ATP of 245 ± 20 nM (GST−cdk2) and 272 ± 15 nM (GST−cdk7), confirming that the GST tag at the N-terminus of cdks does not interfere with the binding of nucleotides.

The change of intrinsic fluorescence related to the binding of ATP was also useful in defining the stoichiometry of binding as well as the active fraction of the cdk preparations used. A value of 0.9 mol of ATP/1 mol of cdks was obtained for each of the three kinases with the cdk sample used in Figure 2B, indicating that the nucleotide binding site of the cdk preparations was correctly folded with a stoichiometry of one nucleotide binding site per cdk.

Binding of Fluorescently Labeled Nucleotides to Cdks. The fluorescence of mant-derived nucleoside (mant-) has been extensively used to investigate the kinetics and the stoichiometry of nucleotide binding to enzymes. Recently, this approach was extended to the characterization of protein kinases (Rittinger et al., 1996; Rossi et al., 1996). In the present work fluorescent properties of the mant-group were used to quantify the interaction of mant-ATP and mant-ADP with different cdks as well as the formation of cdk−cyclin complexes. The binding of mant-ATP or mant-ADP was monitored both by the quenching of the intrinsic fluorescence of cdks and by the enhancement of mant-fluorescence. The binding of mant-ATP to cdks resulted in a 57% quenching

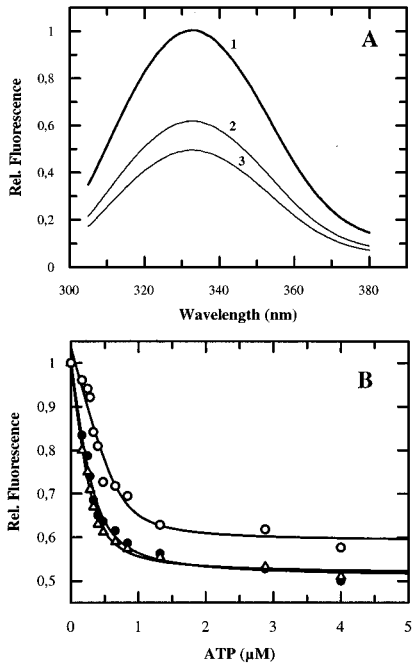

FIGURE 2: Binding titration of ATP to cdks. (A) Emission fluorescence spectrum of cdk2 (0.2 μM) in the absence of nucleotide (1) and in the presence of a saturating concentration (1 μM) of ATP (2) and mant-ATP (3). The excitation was performed at 295 nm. (B) The binding of ATP to cdk2, cdk7, and His_6-cdc2 was monitored by following the quenching of intrinsic Trp-fluorescence of cdks at 340 nm upon excitation at 290 nm. A fixed concentration (0.2 μM) of cdk2 (●), cdk7 (○), and His_6-cdc2 (△) was titrated with increasing ATP concentrations. The data were fitted according to the eq 1, which describes the binding of ATP to a single site within the cdks.

of the intrinsic fluorescence of the kinases (Figure 2A, curve 3) and a 10-fold increase in the fluorescence of the mant-nucleotide, reflecting the highly hydrophobic environment of the cdk's active site. The titration curves of cdks with mant-ATP and mant-ADP as monitored by fluorescence enhancement are shown in Figure 3, panels A and B. The kinases were added incrementally at a constant concentration of mant-nucleotide (0.2 μM) and the curve fitting yielded K_d values of 278 ± 31, 324 ± 27, and 281 ± 30 nM for cdk2, cdk7, and His_6-cdc2, respectively. These values are close to those obtained using intrinsic fluorescence to monitor nucleotide binding (Table 1). As already observed with intrinsic fluorescence titration, the affinity of mant-ADP is 10-fold lower than for mant-ATP and neither the presence of the GST tag on cdk2 or cdk7 nor Mg^{2+} affected the affinity of cdks for the nucleotide. Moreover, mant-ATP was fully displaced when an excess of ATP was added and displacement titrations (Figure 3C) yielded K_d values for ATP on the order of 300 nM. These results confirm that both types of signals monitor the same process and that the fluorescent group attached at the 2′ or 3′ hydroxyl group of the sugar moiety of the ATP does not affect the binding to cdks.

Interaction of Cyclins with Cdks. The term of "unusual" cyclin was used arbitrarily to describe the formation of cdk−cyclin complexes other than the naturally occuring forms isolated *in vivo*. The formation of "usual" and "unusual" cdk−cyclin complexes was monitored and quantified both by enhancement of fluorescence of mant-ATP bound to cdks and by inhibition of mant-ATP displacement by an excess of unlabeled nucleotide (Table 2). Moreover, these results correlated directly with the fraction of stable cdk−cyclin complexes estimated for each titration using size-exclusion HPLC and identified by SDS−PAGE.

Binding of Cyclins to Cdks as Monitored by mant-ATP Fluorescence. The binding of cyclin A to cdk2 and His_6-cdc2 or of cyclin H to cdk7 resulted in a 3-fold increase in the fluorescence of the mant-ATP previously bound to the kinase without a shift in the emission spectrum. The titration curves obtained by enhancement of mant-ATP fluorescence (Figure 4A) follow a monophasic pattern, and their fitting yields K_d values of 48 nM (cdk2−cyclin A), 52 nM (cdk7−cyclin H), and 88 nM (His_6-cdc2−cyclin A) with a 1/1 (cyclin−cdk) stoichiometry for all the complexes. The formation of unusual complexes (cdk2−cyclin H, cdk7−cyclin A, and cdc2−cyclin H) also induced a 3-fold enhancement of the mant-ATP fluorescence (Figure 4B), and the dissociation constants (in a 1−2 μM range) were at least 15−25-fold higher compared to those obtained for the complexes formed with the natural cyclin partner (Table 2). Titration of the bound nucleotide performed by reverse phase HPLC at saturating concentrations of cyclin as already described (John et al., 1990; Divita et al., 1993a) yielded a 1/1 ratio of mant-ATP bound per cdk−cyclin complex. This confirms that the enhancement of mant-ATP fluorescence was indeed mainly due to a dramatic conformational change in the nucleotide binding site of the cdks and not instead associated with a release of the nucleotide.

Binding of Cyclins to Cdks as Monitored by Size-Exclusion HPLC. The monomers (cdks or cyclins) and the different cdk−cyclin complexes were separated by size-exclusion HPLC using a 200 mM phosphate buffer at pH 6.8, as described in Experimental Procedures. Cyclin H, cdks, cyclin A, and the cdk−cyclin complexes were eluted at 17, 16, 15, and 13 min, respectively. As shown in Figure 5 (panels A and B), after 15 min incubation of cdk2 with cyclin A or cdk7 with cyclin H in an equimolar ratio (0.2 μM) in the presence of 2 μM ATP, cdks were fully complexed with their cyclin partner, thus well in accordance with a 1/1 (cdk−cyclin) stoichiometry. Only one peak (13 min) was detected, corresponding to the retention time of the cdk−cyclin complex, and no higher molecular weight species were noted. In the absence of ATP, only 75% of the monomers were engaged in a complex, indicating that the stability of the cdk−cyclin complexes formed was dependent on the presence of nucleotide. At higher concentrations of cyclins (3 μM), the different complexes cdk2−cyclin H, His_6-cdc2−cyclin H, and cdk7−cyclin A were also detected by size-exclusion HPLC and identified by gel electrophoresis (Figure 5C). Figure 5D shows a cyclin H concentration-dependent titration of the formation of the cdk2−cyclin H complex as monitored by size-exclusion HPLC. The titration curve follows a monophasic pattern and the best fit yields a K_d value of 0.94 μM for the cdk2−cyclin H complex. These data correlate perfectly with the lower affinity observed for unusual complexes by fluorescence titrations.

Binding of Cyclins to Cdks as Monitored by Displacement Experiments. Mant-ATP bound to cdks can be fully displaced by an excess of unlabeled nucleotide, resulting in a 10-fold decrease in the fluorescence of the mant-group. The dissociation rate of mant-ATP from cdk2 using a 200-fold excess of ATP can be kinetically estimated by fitting the time-dependent curve (Figure 6A) as a single exponential to a rate constant of (k_{obs}) 5.4 × 10^{-3} s^{-1}. In the presence

Table 1: Affinity Constants [K_d (μM)] of Cdks for Nucleotides and Fluorescent Analogues[a]

	cdk2		cdk7		cdc2	
nucleotides	monomer	+ cyclin A	monomer	+ cyclin H	monomer	+ cyclin A
ATP	0.227 ± 0.02		0.28 ± 0.02		0.234 ± 0.03	
ADP	1.4 ± 0.4		2.7 ± 0.3		2.1 ± 0.5	
mant-ATP	0.278 ± 0.03	0.075 ± 0.01	0.324 ± 0.027	0.087 ± 0.012	0.281 ± 0.030	0.072 ± 0.007
mant-ADP	1.7 ± 0.5	2.0 ± 0.5	3.1 ± 0.8	1.8 ± 0.4	2.3 ± 0.7	1.4 ± 0.2

[a] K_d values were determined by monitoring either the quenching of intrinsic fluorescence of cdks or the enhancement of mant-ATP and mant-ADP fluorescence.

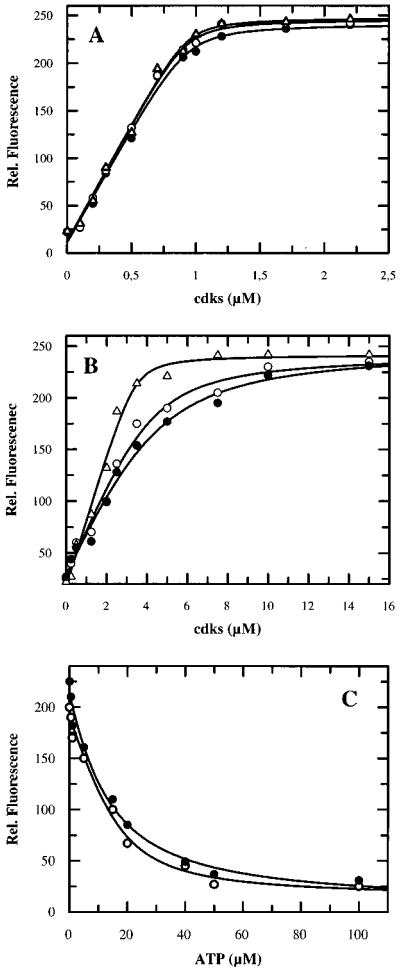

FIGURE 3: Titration of cdk2, cdk7, and His_6-cdc2 with mant-nucleotide. A fixed concentration of mant-ATP or mant-ADP (0.2 μM) was titrated with increasing concentration of cdk2 (●), cdk7 (○), and His_6-cdc2 (△). The binding of mant-ATP (panel A) or mant-ADP (panel B) was monitored by following the enhancement of the mant-group fluorescence at 440 nm upon excitation at 350 nm, and the data were fitted as described in Figure 2. (C) Displacement of mant-ATP from cdk7 (○) and His_6-cdc2 (●) by ATP. Cdks (0.1 μM) were previously incubated in the presence of mant-ATP (0.8 μM) and titrated by increasing ATP concentrations.

of an equimolar concentration of cyclin A, the dissociation rate of mant-ATP from cdk2 is reduced to a value of 1.2×10^{-3} s^{-1}. Cyclins behave as nucleotide dissociation inhibitors since the release of nucleotide from cdks induced by an excess of ATP is decreased upon addition of cyclin (Figure 6A). The displacement kinetics of mant-ATP from cdks by an excess of ATP is similar for the three cdks analyzed (ca. 5×10^{-3} s^{-1}), and a 5-fold decrease in the rate of mant-ATP release from the cdk−cyclin complex is observed with both cyclin H and cyclin A.

Table 2: Affinity Parameters of the Different Cdk−Cyclin Complexes[a]

	cyclin A		cyclin H	
	K_{d1} (nM)	K_{d2} (nM)	K_{d1} (nM)	K_{d2} (nM)
cdk2	48 ± 7	55 ± 7	1200 ± 48	1450 ± 85
cdk7	824 ± 11	750 ± 24	52 ± 7	61 ± 10
cdc2	88 ± 5	78 ± 5	1700 ± 210	1810 ± 100

[a] K_{d1} and K_{d2} were determined by direct titration using the enhancement of the mant-ATP fluorescence and by mant-ATP displacement experiments, respectively.

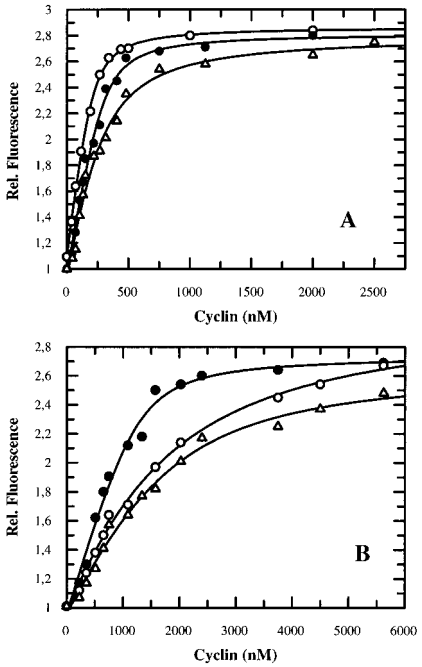

FIGURE 4: Binding titration of cyclins to cdks followed by mant-ATP fluorescence enhancement. Cdks (0.2 μM) previously saturated with mant-ATP (1 μM) were titrated with increasing amounts of cyclin A or cyclin H. The enhancement of mant-ATP fluorescence was monitored at 450 nm upon excitation at 340 nm. (A) Titration curves for "usual" cdk2−cyclin A (○), cdk7−cyclin H (●), and cdc2−cyclin A (△) complexes. (B) Titration curve of the "unusual" cdk2−cyclin H (○), cdk7−cyclin A (●), and cdc2−cyclin H (△) complexes. Both experiments were fitted using quadratic equation.

The inhibitory effect of cyclin on ATP release was used as an alternative for the quantitative analysis of complex formation between cdks and cyclins, by following the dissociation rate constants of fluorescently labeled ATP from cdks. Mant-ATP was first bound to the cdk, using a 5-fold excess compared to the K_d value. The dissociation of mant-ATP from cdks with an excess of nonlabeled ATP (300 μM) was then measured in the presence of increasing concentrations of the cyclin partner. The fluorescence decay kinetics were fitted according to a single exponential which yielded the rate constant for dissociation of mant-ATP (k_{obs}).

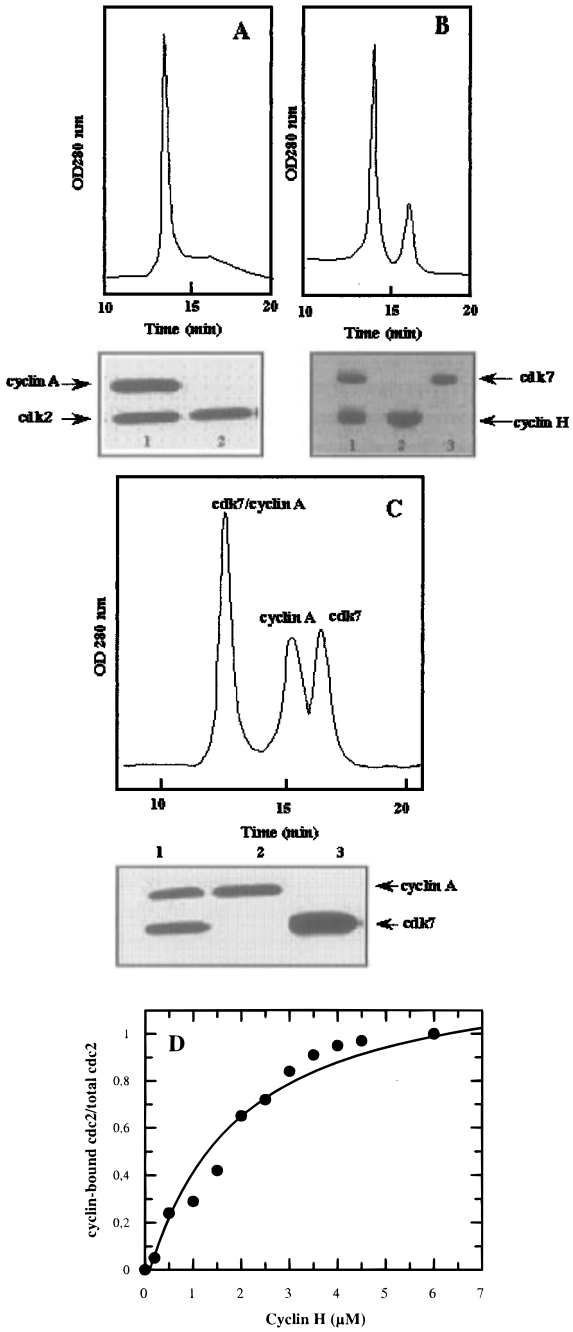

FIGURE 5: Separation of cdk−cyclin complexes by size-exclusion HPLC. Cdks and cyclins (0.2 μM) were preincubated 15 min in a phosphate buffer pH 6.8 and applied onto two size-exclusion HPLC columns in series. The elution was performed with phosphate buffer at a flow rate of 0.8 mL/min, and the different peaks were analyzed by SDS−PAGE. (A) Separation of the cdk2−cyclin A complex. Lane 1, peak 1 (cdk2−cyclin A) and lane 2, purified cdk2. (B) Separation of the cdk7−cyclin H complex. Lane 1, peak 1 (cdk7−cyclin H); lanes 2 and 3, purified cyclin H and cdk7. (C) Separation of the cdk7−cyclin A complex. Lane 1, peak 1 (cdk7−cyclin A); lane 2, peak 2 (cyclin A); and lane 3, peak 3 (cdk7). (D) Titration curve of cdc2 with cyclin H as "unusual" cyclin partner. Cdc2 (0.2 μM) was incubated with increasing concentration of cyclin H (0−10 μM) and applied onto size-exclusion HPLC columns. The dimeric fraction (cdc2−cyclin H) was quantified by size-exclusion chromatography.

According to the model presented in Scheme 1, the rate constants k_{+1} and k_{+2} are negligible considering the large excess of unlabeled nucleotide. The rate constant k_{obs} is therefore composed of two components: the dissociation of the nucleotide from the monomer cdk (k_{-1}) and its dissociation from the cdk−cyclin complex (k_{-2}). Since the rate k_{-2} cannot be determined precisely, the dissociation of the nucleotide from cdks in the absence of cyclin must be fast in comparison with the dissociation from the cdk−cyclin complex and k_{-2} is negligible compared to k_{+1}, which is more than 1 order of magnitude faster.

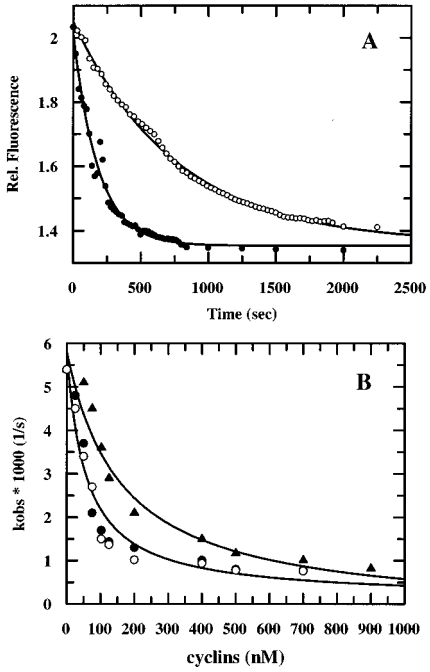

FIGURE 6: Interaction of cdks with cyclins monitored by nucleotide release experiments. (A) The mant-ATP displacement from cdk2 (0.1 μM) by a 200-fold excess of ATP was monitored in the absence (●), and in the presence (○) of an equimolar cyclin A concentration. The decrease of the mant-ATP fluorescence was monitored at 450 nm and the kinetic was fitted as single exponential. (B) The displacement of mant-ATP/cdk2 (○), mant-ATP/cdc2 (▲), and mant-ATP−cdk7 (●) complexes was titrated by adding cyclin A and cyclin H concentrations, respectively. The data were fitted as single exponential and the observed dissociation rate constants (k_{obs}) were analyzed as a function of cyclin concentrations. The data were fitted to eq 2 to yield K_d values of 55, 61, and 78 nM for the cdk2−cyclin A, cdk7−cyclin H, and cdc2−cyclin A complexes.

Scheme 1

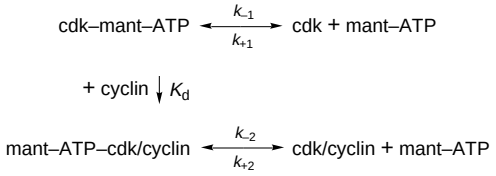

Figure 6B shows the variation of the dissociation rate constant of mant-ATP depending on the concentration of the cyclin used. The dissociation data (k_{obs}) were fitted as described in the Experimental Procedures to dissociation constant values of 55 nM (cdk2−cyclin A), 61 nM (cdk7−cyclin H), and 78 nM (cdc2−cyclin A), which are quite similar to those calculated by direct fluorescence titration. The binding of unusual cyclins to cdks also reduced the rate of mant-ATP displacement therefore leading to lower affinity constants of 1.8 μM (cdc2−cyclin H), 0.75 μM (cdk7−cyclin A), and 1.45 μM (cdk2−cyclin H) compared to the natural cyclin partner. It should be noted that the formation of the cdk−cyclin complexes was not affected by the presence of 200 mM phosphate, which validates the HPLC size exclusion method to monitor the formation of these cdk−cyclin complexes.

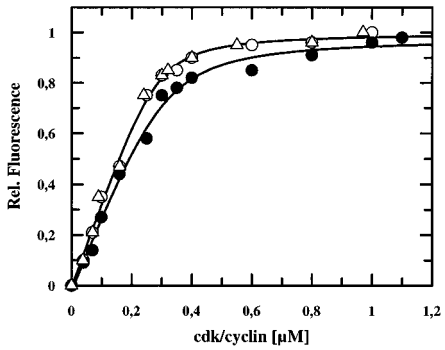

FIGURE 7: Titration of cdk2−cyclin A, cdk7−cyclin H, and His_6-cdc2−cyclin A with mant-ATP. A fixed concentration of mant-ATP (0.2 μM) was titrated with increasing amount of cdk7/cyclin H (●), His_6-cdc2/cyclin A (○), and cdk2/cyclin A (△) complexes purified by size-exclusion chromatography. The enhancement of the fluorescence of the mant-ATP was monitored at 440 nm and the curves fitting was performed as described in the Figure 3.

In the absence of cyclin, the rate constant of mant-ADP release from cdc2 by addition of an excess of ADP is 2-fold faster than that of mant-ATP. In contrast to the result observed for mant-ATP, the displacement of mant-ADP with an excess of ADP was not dramatically affected upon cyclin binding, which suggests that the conformational change induced in the cdk upon cyclin binding affects the organization of the phosphate group rather than the adenine moiety of the nucleotide bound to cdk.

Binding of Nucleotides to the Cdk−Cyclin Complexes. The binding of ATP and ADP to cdk−cyclin complexes was monitored using the large enhancement of the mant-labeled nucleotide fluorescence which occurs upon binding to cdks. The cdk2−cyclin A, cdk7−cyclin H, and cdc2−cyclin A complexes were formed and checked as to their homogeneity by size-exclusion HPLC. The binding of mant-ATP to preformed cdk−cyclin complexes resulted in a 15-fold increase in mant-ATP fluorescence. The titration curves shown in Figure 7 are monophasic, and their fitting yields mant-ATP dissociation constant values of 75 ± 10 nM for cdk2−cyclin A, 87 ± 12 nM for cdk7−cyclin H, and 72 ± 7 nM for cdc2−cyclin A complexes. These affinities for ATP are at least 3-fold higher than those obtained for free cdks. In contrast, the affinity of these cdk−cyclin complexes for mant-ADP is in the same range as that obtained for the cdks alone with K_d values of 2.0 ± 0.5, 1.8 ± 0.4, and 1.4 ± 0.2 μM for cdk2−cyclin A, cdk7−cyclin H, and cdc2−cyclin A, respectively (Table 1).

DISCUSSION

In the present work, we have successfully applied fluorescence technology using both fluorescently labeled nucleotides and intrinsic fluorescence of cdks to further the understanding of the mechanism and the different parameters which control the formation of nonphosphorylated cdk−cyclin complexes. We have characterized the interaction of three different cdks, cdc2, cdk2, and cdk7, with cyclins A and H, both in usual and unusual complexes, the former relating to complexes observed and isolated *in vivo*, as opposed to the latter. Cdc2, cdk2, and cyclin A were chosen as the most extensively studied and representative members of the cdk−cyclin family, the kinase activity of which varies in a cyclical fashion (Norbury & Nurse, 1992). The cdk7−cyclin H complex was chosen for its differences compared to other cdk−cyclin complexes, first in that it forms a trimeric complex with the additional MAT1 subunit and second in its constitutive activity throughout the cell cycle (Fesquet et al., 1993; Poon et al., 1993; Solomon et al., 1993; Devault et al., 1995; Fisher et al., 1995; Tassan et al., 1995).

Nucleotide Binding to Monomeric Cdks. All cdks contain three highly conserved and strategically located Trp-residues (locations 167, 187, and 229 in cdk2, see Figure 1). Trp167 is located in the so-called T-loop motif (residues 152−170), which contains the essential Thr160 phosphorylation site, interacts directly with the ATP binding site, and controls the accessibility of the protein substrate (Radzio-Andzelw et al., 1995; Johnson et al., 1996). Trp187 is involved in cyclin A binding and Trp229 in the interaction of cdks with small proteic "regulator" $p9^{cksHs1}$ (Bourne et al., 1996). These three deeply buried Trp-residues confer a characteristic intrinsic fluorescence to cdks, which is extremely sensitive to the binding of nucleotides to cdks.

Our experiments show that cdk2, cdk7, and cdc2, exhibit a relatively high and similar affinity for ATP in the order of 300 nM, whereas the affinity of these cdks for ADP is ca.10-fold lower (Table 1). Moreover, we find that, although the catalytic substrate of cdks is the ATP−Mg complex, the binding of ATP is not dependent on the presence of $MgCl_2$, which can be explained by the inactive organization of the catalytic site of monomeric cdks in the absence of a cyclin partner. These results demonstrate that the cdks can bind ATP with high affinity in a structural orientation which is inconsistent with phosphate transfer reactions. Similar values defining a strong affinity for ATP have also been reported for other protein kinases, including the catalytic subunit of cPKA (Herberg & Taylor, 1993), epidermal growth factor receptor protein tyrosine kinase (Cheng & Koland, 1996), and isocitrate dehydrogenase kinase/phosphatase (Rittinger et al., 1996). Mant-ATP analogs bind the catalytic site of cdks with high affinity (K_d ca. 300 nM) in the same range as ATP, indicating that the labeled group attached to the sugar moiety of ATP does not alter the binding ability. This is not surprising considering that, in the cdk2−ATP complex, the 2′ and 3′ hydroxyl groups of the sugar do not interact with residues in the catalytic site of the kinase (Debondt et al., 1993).

All protein kinases share a high degree of homology with well-defined domains, and a common architecture composed of two lobes, the smaller associated with ATP-binding domain and the larger containing the substrate binding domain, between which the active site cleft is located [Reviews: Radzio-Andzelm et al. (1995), Johnson et al. (1996)]. On the basis of our results, we can now extend this homology to the nucleotide binding process and to the related conformational change. Indeed, as cdks and the active forms of the other kinases share a similar high affinity for ATP, we conclude that the essential phosphorylation of cdks on the T-loop threonine (which occurs upon activation of the kinase by CAK) does not seriously interfere with the binding of ATP, but that it is instead required for the catalytic process. Mutation of the essential threonine residue Thr161 on cdc2 (Atherton-Fessler et al., 1993) and of Thr196 on cPKA (Adams et al., 1995) has lead to a similar conclusion: phosphorylation is required for the phosphoryl transfer reaction but does not interfere with the affinity either for the nucleotide or for the substrates.

Cyclin Binding to Cdk Induces a Change in the Conformation of the Nucleotide Binding Site. Using mant-ATP fluoresence, we have monitored kinetically whether any conformational changes occur in the nucleotide binding site of cdk upon cyclin binding. Our kinetics clearly show that binding of a cyclin subunit to a cdk induces a 3-fold increase in the affinity for ATP, but not for ADP, which is coupled to a decrease in nucleotide release from the cdk subunit.

Together, the increase in mant-ATP fluorescence and the decrease in nucleotide exchange upon binding of a cyclin to a cdk provide evidence for an important conformational change in the nucleotide binding site and in the catalytic cleft. The fact that the affinity of cdks for ADP remains unchanged upon cyclin binding clearly denotes that this conformational change occurs close to the $\gamma-\beta$ phosphate bond of the nucleotide, as already suggested from the structures of cdk2 and of the cdk2−cyclin A complex. Upon binding of the cyclin subunit, the ATP site is reconfigured and the PSTAIRE helix moves into the catalytic site by rotation thus placing the catalytic residues and the $\beta-\gamma$ phosphate bond of ATP correctly, turning it into an appropriate conformation for nucleophilic attack from a bound substrate (Debondt et al., 1993; Jeffrey et al., 1995). On the basis of these results, we suggest that binding of cyclin to a cdk increases the affinity for ATP by reducing the off-rate of ATP.

Mechanism of Formation of the Cdk−Cyclin Complexes. Cyclin binding is an absolute prerequisite to the activation of cdks, as it promotes the phosphorylation of the conserved threonine at the active site, itself essential for the full activation of cdks. The X-ray cristallographic structure of the cdk2−cyclin A complex has provided some clues for understanding these mechanisms of cdk regulation from a structural point of view (Jeffrey et al, 1995; Radzio-Andzelm et al., 1995; Johnson et al., 1996; Russo et al., 1996).

We have used the high sensitivity of mant-labeled nucleotide to quantify the formation of the cdk−cyclin complexes at the molecular and dynamic levels and to monitor the conformational change which occurs in the catalytic site of cdks upon binding of cyclin to the cdk. Binding of cyclins to cdks resulted in a 2-fold increase of fluorescence of the mant-ATP bound to cdks and reduced dramatically the rate of mant-ATP displacement from the cdks by an excess of ATP.

Cdc2, cdk2, and cdk7 exhibit a high affinity for their corresponding cyclin A or cyclin H partners with dissociation constant values of ca. 50 nM obtained in the presence of ATP, whichever the quantitative method used. As the binding of the cyclin with the cdk is identical for the three complexes studied, the mechanism of interaction must be common to all cdk−cyclin complexes. Given the tight interaction occurring between cdks and cyclins, phosphorylation of the conserved Thr161 of cdks is obviously not an absolute prerequisite for the formation of cdk−cyclin complexes. Our results are further supported by the fact that the nonphosphorylated cdk2−cyclin A and cdc2−cyclin B complexes have been isolated *in vitro* (Desai et al., 1995) and shown to be partially active (Connell-Crowley et al., 1993). In contrast, the presence of nucleotide stabilized the cdk−cyclin complexes. Moreover, from the structural data of the cdk2−cyclin A complex, it seems clear that accessibility of Thr160 for phosphorylation by CAK is only promoted following binding of cyclin A (Jeffrey et al., 1995). The recent determination of the structure of the phosphorylated cdk2−cyclin A complex confirms that phosphorylation on the Thr160 of cdk2 improves the effect of the cyclin by maintaining the T-loop in the catalytic cleft and stabilizing the cdk−cyclin complexes in a more active conformation (Russo et al., 1996). Finally, in the case of the cdk7−cyclin H complex, neither phosphorylation on Thr176 (corresponding to Thr160 on cdc2) nor binding of MAT the third component of CAK is essential for the basic interactions between the cdk and cyclin components, but nevertheless plays a role in their stabilization (Devault et al., 1995; Fisher et al., 1995).

With the high sensitivity of the mant-fluorescent probe used for the first time, we have observed that cdks can form dimeric complexes with cyclins other than their usual cyclin partner. Indeed cdk2−cyclin H, cdc2−cyclin H, and cdk7−cyclin A complexes were isolated *in vitro* by size-exclusion HPLC and identified by gel electrophoresis. The stability of these cdk−cyclin complexes at high salt concentration (up to 400 mM) indicates that the interface between the two subunits is mainly formed of hydrophobic interactions, which clearly play a central role in the stability of the cdk2−cyclin A complex. Of interest, however, cdks exhibit a 25−50-fold lower affinity for an unusual cyclin partner than for their usual cyclin partner. Thermodynamically, the usual and unusual cdk−cyclin complexes are not drastically different. Indeed this difference lower than 2 kcal/mol must correspond only to few interactions. The binding of cyclin H to cdk2 or cdc2 and of cyclin A to cdk7 produces the same 2-fold increase in the fluorescence of mant-ATP bound to cdks which suggests that the formation of unusual complexes involves the same type of interactions as those described for the usual complexes. The X-ray structure of cdk2−cyclin A complex shows that binding of cyclin occurs on one side of the cdk and that the main contact between cdk2 and cyclin A involves the α1-helix (containing the PSTAIRE motif) and the T-loop of the cdk2 and the α3−, α4-, and α5-helices of the cyclin A. Several residues implicated in this interface between cdk2 and cyclin A appear to be conserved in all cdks and cyclins, including the PSTAIRE helix in Figure 1 and mainly two invariant residues located in the α3- and α5-helices of conserved cyclin helical fold, Lys266 and Glu295. Preliminary kinetic experiments for cyclin−cdk binding have revealed that the formation of cdk−cyclin complexes occurs in at least two steps, in which the cdk−cyclin association rate is similar for usual and unusual complexes (unpublished results). Taking together the structural information and our kinetic results, we propose that the first step in the cdk−cyclin interaction involves the PSTAIRE helix of cdk and the α3- and α5-helices of the cyclin irrespective of the cyclin and the cdk type. Additionally, selectivity of binding most likely arises from stabilization of a complex between a specific cdk and cyclin by other contacts between the two subunits. Moreover, phosphorylation of the essential Thr160 of a cdk increases the stability of "chimeric" cdk−cyclin complexes as has already been suggested for cdc2−cyclin A (Atherton-Fessler et al., 1993; Desai et al., 1995).

The formation of a such chimeric complexes *in vitro* raises the question of their biologically relevant role in the regulation and progression of the cell cycle. The specificity of cdk−cyclin partnerships at a particular point in the cell cycle is in part regulated by temporal expression and

degradation patterns of cdks and cyclins. Moreover, many biological situations suggest that additional mechanisms may exist in the cell that prevent temporally inappropriate activation of the cdk kinases. Proteins other than cdks and cyclins, such as the so-called cyclin-dependent kinase inhibitors (Zhang et al., 1994) and post-translational modifications, are most likely involved in the stability and regulation of cdk−cyclin complexes (Kobayashi et al., 1991).

ACKNOWLEDGMENT

We acknowledge Dr. S. H. Kim for providing the cdk2 coordinates, Drs. L. H. Tsai and J. Shuttleworth for providing the GST constructs, and Dr. J. A. Endicott for helpful discussions.

REFERENCES

Adams, J. A., McGlone, M. L., Gibson, R., & Taylor, S. S. (1995) *Biochemistry 34*, 2447−2454.
Atherton-Fessler, S., Parker, L. L., Geahlen, R. L., & Piwnica-Worms, H. (1993) *Mol. Cell. Biol. 13*, 1675−1685.
Bagby, S., Kim, S., Maldonado, E., Tong, K. I., Reinberg, D., & Ikura, M. (1995) *Cell 82*, 857−867.
Bazan, F. J. (1996) *Proteins 24*, 1−17.
Bossemeyer, D. (1994) *Trends Biochem. Sci. 19*, 201−205.
Bourne, Y., Watson, M. H., Hickey, M. J., Holmes, W., Rocque, W., Reed, S. I., & Tainer, J. A. (1996) *Cell 84*, 863−874.
Brown, N. R., Noble, M. E., Endicott, J. A., Garman, E. F., Wakatsuki, S., Mitchell, E., Rasmussen, B., Hunt, T., & Johnson, L. N. (1995) *Structure 3*, 1235−1247.
Cheng, K., & Koland, J. C., (1996) *J. Biol. Chem. 271*, 311−318.
Connell-Crowley, L., Solomon, M. J., Wei, N., & Harper, J. W. (1993) *Mol. Biol. Cell. 4*, 79−92.
De Bondt, H. L., Rosenblatt, J., Jancarik, J., Jones, H. D., Morgan, D. O., & Kim, S. H. (1993) *Nature 363*, 595−602.
Desai, D., Wessling, H. C., Fisher, R. P., & Morgan, D. O. (1995) *Mol. Cell. Biol. 15*, 345−350.
Devault, A., Martinez, A. M., Fesquet, D., Labbe, J. C., Morin, N., Tassan, J. P., Nigg, E. A., Cavadore, J. C., & Doree, M. (1995) *EMBO J. 14*, 5027−5036.
Divita, G., Jault, J.-M., Gautheron, D. C., & Di Pietro, A. (1993a) *Biochemistry 32*, 1017−1024.
Divita, G., Goody, R. S., Gautheron, D. C., & Di Pietro, A. (1993b) *J. Biol. Chem. 268*, 13178−13186.
Dunphy, W. G. (1994) *Trends Cell. Biol. 4*, 202−207.
Fesquet, D., Labbe, J. C., Derancourt, J., Capony, J.-P., Galas, S., Girard, F., Lorca, T., Shuttleworh, J., Doree, M., & Cavadore, J. C. (1993) *EMBO J. 12*, 3111−3121.
Fisher, R. P., & Morgan, D. O. (1994) *Cell 78*, 713−724.
Fisher, R. P., Jin, P., Chamberlin, H. M., & Morgan, D. O. (1995) *Cell 83*, 47−57.
Hanks, S. K., Quinn, A. M., & Hunter, T. (1988) *Science 241*, 42−52.
Herberg, F. W., & Taylor, S. S. (1993) *Biochemistry 32*, 14015−14022.
Hiratsuka, T. (1983) *Biochim. Biophys. Acta 742*, 496−508.
Hubbard, S. R., Wei, L., Ellis, L., & Hendrickson, W. A. (1994) *Nature 372*, 746−754.
Hunter, T., & Pines, J. (1994) *Cell 79*, 573−582.
Jeffrey, P. D., Russo, A. A., Polyak, K., Gibbs, E., Hurwitz, J., Massagué, J., & Pavletich, N. P. (1995) *Nature 376*, 313−320.
John, J., Sohmen, R., Feuerstein, J., Linke, R., Wittinghofer, A., & Goody, R. S. (1990) *Biochemistry 29*, 6958−6965
Johnson, L. N., Noble, M. E. M., & Owen, D. J. (1996) *Cell 85*, 149−158.
Knighton, D. R., Zheng, J., Ten Eyck, L. F., Ashford, V. A., Xuong, N. H., Taylor, S. S., & Sowadski, J. M. (1991) *Science 253*, 407−414.
Kobayashi, H., Stewart, E., Poon, R., Adamczewski, J. P., Gannon, J., & Hunt, T. (1992) *Mol. Biol. Cell. 3*, 1279−1294.
Labbe, J. C., Martinez, A. M., Fesquet, D., Capony, J. P., Darbon, J. M., Derancourt, J., Devault, A., Morin, N., Cavadore, J. C., & Doree, M. (1994) *EMBO J. 13*, 5155−5164.
Laemmli, U. K. (1970) *Nature 227*, 680−685.
Longenecker, K. L., Roach, P. J., & Hurley, T. D. (1996) *J. Mol. Biol. 257*, 618−631.
Lorca, T., Labbé, J.-C., Devault, A., Fesquet, D., Capony, J.-P., Cavadore, J.-C., Le Bouffant, F., & Dorée, M. (1992) *EMBO J. 11*, 2381−2390.
Maridor, G., Gallant, P., Golsteyn, R., & Nigg, E. A. (1993) *J. Cell Sci. 106*, 535−544.
Morgan, D. O. (1995) *Nature 374*, 131−134.
Nikolov, D. B., Chen, H., Halay, E. D., Usheva, A. A., Hisatake, K., Lee, D. K., Roeder, R. G., & Burley, S. K. (1995) *Nature 377*, 119−128.
Norbury, C., & Nurse, P. (1992) *Annu. Rev. Biochem. 61*, 441−470.
Pines, J. (1993) *Trends Biochem. Sci. 18*, 195−197.
Pines, J., & Hunter, T. (1991) *J. Cell Biol. 115*, 1−17.
Poon, R. Y. C., Yamashita, K., Adamczevski, P., Hunt, T., & Suttleworth, J. (1993) *EMBO J. 12*, 3123−3132.
Radzio-Andzelm, E., Lew, J., & Taylor, S. (1995) *Structure 3*, 1135−1141.
Rittinger, K., Negre, D., Divita, G., Scarabel, M., Bonod-Bidaud, C., Goody, R. S., Cozzone, A. J., & Cortay, J.-C. (1996) *Eur. J. Biochem. 237*, 247−254.
Rossi, F., Labourier, E., Forne, T., Divita, G., Derancourt, J., Riou, J. F., Antione, E., Cathala, G., Brunel, C., & Tazi, J. (1996) *Nature 381*, 80−82.
Russo, A. A., Jeffrey, P. D., & Pavletich N. P. (1996) *Nat. Struct. Biol. 3*, 696−700.
Saraste, M., Sibbald, P. R., & Wittinghofer, A. (1990) *Trends Biochem. Sci. 15*, 430−434.
Sherr, C. J. (1994) *Cell 79*, 551−555.
Solomon, M. J. (1994) *Trends Biochem. Sci. 19*, 496−500.
Solomon, M. J., Harper, J. W., & Shuttleworth, J. (1993) *EMBO J. 12*, 3133−3142.
Tassan, J. P., Schultz, S. J., Bartek, J., & Nigg, E. A. (1994) *J. Cell Biol. 127*, 467−478.
Tassan, J. P., Jaquenoud, M., Fry, A. M., Frutiger, S., Hughes, G. J., & Nigg, E. A. (1995a) *EMBO J. 14*, 5608−5617.
Taylor, S., & Radzio-Andzelm, E. (1994) *Structure 2*, 345−355.
Watanabe, N., Broome, M., & Hunter, T. (1995) *EMBO J. 14*, 1878−1891.
Xu, R. M., Carmel, G., Sweet, R. M., Kuret, J., & Cheng, X. (1995) *EMBO J. 14*, 1015−1023.
Zhang, F., Strand, A., Robbins, D., Cobb, M. H., & Goldsmith, E. (1994) *Nature 367*, 704−711.
Zhang, H., Hannon, G. J., & Beach, D. (1994) *Genes Dev. 8*, 1750−1758.
Zheng, J., Knighton, D. R., Ten Eyck, L. F., Karlsson, R., Xuong, N. H., Taylor, S. S., & Sowadski, J. M. (1993) *Biochemistry 32*, 2154−2161.

BI962349Y